Research Square

Preprints are preliminary reports that have not undergone peer review.
They should not be considered conclusive, used to inform clinical practice,
or referenced by the media as validated information.

Climate hazards and power-system resilience: why heat, hydropower and storms require different indicators

Behzod Tagaev
National University of Uzbekistan named after Mirzo Ulugbek
Yuriy Bilan
LUT-yliopisto: LUT University
Dalia Streimikiene
dalia.streimikiene@lei.lt

Lietuvos energetikos institutas https://orcid.org/0000-0002-3247-9912

Research Article

Keywords: climate adaptation, electricity-system resilience, heat exposure, hydropower shortfall, tropical storms, sustainable energy

Posted Date: October 26th, 2026

DOI: https://doi.org/10.21203/rs.3.rs-10795546/v1

License: This work is licensed under a Creative Commons Attribution 4.0 International License.
Read Full License

Climate hazards and power-system resilience: why heat, hydropower and storms require different indicators

Behzod Tagaev, National University of Uzbekistan named after Mirzo Ulugbek, Tashkent, Uzbekistan
Email: btagaev@nuu.uz
ORCID: 0000-0002-4065-9817

Yuriy Bilan, LUT University, Lappeenranta, Finland
Email: y.bilan@prz.edu.pl
ORCID: 0000-0003-0268-009X

Dalia Streimikiene, Lithuanian Energy Institute, Kaunas, Lithuania
Corresponding author: Dalia Streimikiene; Email: dalia.streimikiene@lei.lt
ORCID: 0000-0002-3247-9912

Abstract. Climate hazards affect electricity systems through different physical channels and at different temporal and spatial scales. This study tests whether internationally comparable monthly data can identify those distinct responses. Two linked panels for 2019–2025 are analysed: a 12-country climate panel with 1,008 country-month observations and a 74-country storm panel with 6,216 observations. Storm tracks from the International Best Track Archive for Climate Stewardship are spatially linked to 34,936 geocoded power plants. Models include country-by-calendar-month and global year-month effects, small-cluster inference, and extensive sensitivity tests. Each additional degree of monthly cooling-threshold exposure above 18 °C is associated with 2.62% higher electricity demand. By contrast, operational hydropower shortfalls do not robustly predict absolute fossil generation or net imports, and tropical-storm exposure does not produce a statistically distinguishable national monthly generation response. These null aggregate estimates should not be interpreted as evidence that droughts or storms cause no disruption. They show that national monthly data capture persistent heat-related pressure more effectively than short, localized outages or restoration processes. The study reframes this asymmetry as a hazard-measurement result and demonstrates that resilience indicators must match each hazard's physical pathway, geographic footprint, and duration. The findings support heat-responsive adequacy planning and higher-resolution monitoring of hydrological and storm risks.

Keywords: climate adaptation; electricity-system resilience; heat exposure; hydropower shortfall; tropical storms; sustainable energy

1. Introduction

Climate exposure has become a central constraint on electricity-system resilience and, consequently, on sustainable development. Higher temperatures increase cooling demand while reducing the usable capacity of generation and network assets. Low water availability limits hydropower and cooling, and tropical storms can damage local infrastructure within hours. These pressures emerge while electricity systems are decarbonizing and incorporating larger shares of weather-sensitive renewable generation. Cross-country evidence also indicates that the relationship between renewable energy use and climate vulnerability differs across high- and low-vulnerability economies, reinforcing the need to account for heterogeneous national contexts (Shahzad et al., 2024). Climate adaptation in the power sector therefore cannot be represented by a single reliability coefficient: it encompasses demand, generation, substitution, interruption, and recovery responses that appear at different spatial and temporal scales. Integrated energy research has quantified the joint exposure of demand and supply to extreme weather (Perera et al., 2020), while high-frequency evidence identifies weather as a major cause of interruptions and restoration delays (Shield et al., 2021).

The development consequences are substantial. Reliable and affordable electricity underpins SDG 7, while adaptation to escalating climate hazards is central to SDG 13. Interruptions reduce firm productivity, disrupt household welfare, constrain essential services, and propagate through supply chains. Electricity price shocks can also generate unequal inflationary effects across countries with different renewable-energy and structural profiles (Vasylieva, Gutowski, et al., 2025). Evidence from Ghana and other developing economies shows that firms respond through self-generation and production adjustment, but these strategies do not eliminate productivity

losses (Abeberese et al., 2021). Causal evidence from an interconnected grid likewise shows that outages materially reduce firm performance (Elliott et al., 2021), while cross-country estimates associate outages with slower economic growth (Chen et al., 2023). Welfare losses are particularly severe where households lack backup power or cannot shift consumption across time (Aweke & Navrud, 2022). Climate-resilient electricity is therefore not solely an engineering objective; it is a condition for inclusive and sustained development.

The physical mechanisms are becoming better understood, but the empirical literature remains fragmented. Heatwaves increase cooling demand while reducing thermal efficiency and network carrying capacity. Drought lowers hydropower generation and can increase fossil generation in other regions through electricity trade (Qiu et al., 2023). Compound dry and hot conditions can connect spring inflow deficits with summer demand peaks, creating prolonged energy droughts rather than isolated monthly disturbances (van der Most et al., 2024). Storms operate through another channel. Wind, precipitation, flooding, and falling vegetation damage local network components and produce restoration processes that may last for days (Li et al., 2025). High-frequency evidence indicates that natural disasters increase both the frequency and duration of outages, with larger effects in poorer localities (Wang et al., 2025).

Renewable expansion does not automatically produce climate resilience. Diversified resources, storage, interconnection, demand response, and firm backup can reduce exposure, but their effectiveness depends on event duration and geographic correlation (Denholm et al., 2021; Schill, 2020; Shen et al., 2025; Zhao et al., 2024; Zheng et al., 2024). Adaptation planning must consequently distinguish between persistent heat pressure, hydrological scarcity, and short but damaging storm events. Treating all three as a common climate shock can obscure the different investments, institutions, and data required to manage them.

A central challenge for adaptation policy is measurement. Direct indicators such as SAIDI, SAIFI, energy not supplied, and forced outage capacity are not available in a consistent global monthly panel. National generation is more widely observed, but it can remain stable when local outages are offset by unaffected plants, imports, reserve generation, or rapid restoration. Aggregate data may therefore reveal persistent system stress and balancing responses without observing the interruption that initiated them. Plant-level evidence confirms that extreme heat and hydrological conditions increase forced outages in Europe, while planned maintenance follows different dynamics (Sergio & Colelli, 2025). Network simulations likewise show that cascading failures depend on the spatial location of vulnerable components and on distributed-generation configurations (Xu et al., 2025a). For sustainable-development monitoring, this creates a consequential risk: apparently stable national supply may coexist with severe local service losses and unequal recovery.

The study contributes to natural-hazards and energy-resilience research in three ways. It compares heat, operational hydropower shortfalls and tropical-storm exposure within a single empirical framework while preserving their distinct physical pathways. It develops an infrastructure-weighted storm measure by spatially linking IBTrACS tracks to power-plant coordinates and mapped capacity. Most importantly, it treats the contrast between a robust heat-demand effect and null monthly hydropower and storm estimates as evidence about measurement scale. Aggregate indicators can identify persistent demand pressure and broad balancing responses, but they cannot substitute for outage, forced-capacity and restoration data when hazards are localized or short-lived. This boundary is consequential for both hazard assessment and adaptation investment.

The objective is to assess how climate-related exposures are associated with observable monthly electricity-system responses and what those associations imply for differentiated adaptation strategies. The analysis asks whether monthly heat exposure raises electricity demand; whether operational hydropower shortfalls are associated with higher absolute fossil generation or net imports as hydropower dependence rises; and whether the share of national generating capacity near a tropical-storm track predicts lower monthly generation. It also tests whether pre-period generation diversification, lagged network losses, and lagged government effectiveness moderate storm exposure. The broader question is whether commonly available cross-country indicators are adequate for designing and monitoring resilient, sustainable electricity systems.

The analysis combines monthly electricity data from Ember with temperature data from CRU TS v4.10, storm tracks from IBTrACS, plant locations from the Global Power Plant Database, network losses from the World Development Indicators, and governance measures from the Worldwide Governance Indicators. The 12-country climate sample contains 1,008 observations, and the 74-country storm sample contains 6,216 observations. The climate sample is an availability sample rather than a statistically representative global sample.

The results are asymmetric across hazards. Heat produces the clearest signal: an additional degree of monthly cooling-threshold exposure is associated with 2.62% higher demand, with leave-one-country-out

estimates ranging from 2.10% to 2.92%. Operational hydropower shortfalls do not robustly predict absolute fossil generation or net imports under Webb inference. Storm-exposure coefficients remain close to zero after potentially post-treatment controls are removed, and isolated event windows show no statistically precise national generation response. Diversification, network-loss, and government-effectiveness interactions are not robust after multiplicity correction. These results imply that climate adaptation should be hazard- and scale-specific. Monthly national data are informative for persistent heat-related demand pressure but insufficient for evaluating short, geographically concentrated outages or restoration performance.

2. Climate hazards, electricity-system resilience and hypothesis development

Temperature affects electricity systems through both demand and supply. The demand response is nonlinear because electricity use increases when temperatures exceed a comfort threshold and cooling equipment is activated. The effect depends on air-conditioning penetration, urban form, income, and the composition of economic activity. Recent system studies show that heatwaves can produce simultaneous increases in electricity demand and reductions in renewable or conventional supply (Xu et al., 2025b). Integrated modeling finds that climate variability creates meaningful reliability gaps when demand and renewable output are evaluated jointly rather than separately (Perera et al., 2020). The effect is especially important during prolonged heat because the load remains high across consecutive days, reducing the time available for maintenance or reserve recovery.

Heat also constrains supply. Thermal plants lose efficiency as ambient temperature rises. Cooling-water limits can force derating or shutdown. Transmission lines and transformers have temperature-sensitive ratings. Plant-level European evidence identifies a positive relationship between extreme heat and forced outages at thermal generators (Sergio & Colelli, 2025). Research on distribution networks also shows that local warming changes failure risk and component loading (Guddanti et al., 2025). These supply constraints occur at the same time that household and commercial cooling demand increases. The joint movement of demand and available capacity is the central reason heat is treated as a reliability shock rather than merely a consumption determinant.

Monthly data cannot capture hourly peak load or daily cooling degree days, but they can indicate whether an unusually warm month requires persistently higher electricity demand. The analysis therefore uses monthly cooling-threshold exposure and a country-specific 90th-percentile indicator. Both coefficients are expected to be positive.

H1. Higher monthly cooling-threshold exposure increases electricity demand. A month above the country-specific 90th percentile of temperature is associated with higher demand after controlling for country-specific seasonality and global year-month shocks.

Physical drought affects electricity systems through precipitation, snowpack, runoff, reservoir inflow, and storage. The available cross-country panel does not observe that full sequence. The operational hydropower shortfall used here begins only after low hydro output is evident in the power balance, so it can describe contemporaneous substitution but cannot identify a causal effect of meteorological drought.

The substitution can cross borders. Qiu et al. (2023) show that drought in the western United States increases fossil generation and associated emissions in regions beyond the directly affected hydropower area. This spatial transmission is consistent with a networked electricity market in which a local hydrological shock alters dispatch elsewhere. European evidence similarly shows that low spring inflows can increase the probability of prolonged summer energy droughts when heat raises demand simultaneously (van der Most et al., 2024). Hydropower therefore creates both resilience and exposure. It is dispatchable under normal water conditions, but its flexibility becomes scarce during a persistent basin-wide drought.

The substitution response should increase with structural dependence on hydropower. A system with almost no hydro capacity can experience low hydro output without a material aggregate response. A system where hydro supplies a large share must replace a larger amount of dispatchable output. Absolute fossil generation may rise where thermal assets are available. Net imports may rise where interconnection and neighboring supply permit. Outcomes are measured in volumes rather than generation shares so that a lower hydro denominator does not mechanically raise the fossil outcome.

H2. A larger operational hydropower shortfall is associated with higher absolute fossil generation and higher net imports. Both positive associations become stronger as long-run hydropower dependence increases.

Tropical storms damage electrical systems primarily through network infrastructure. High wind can break poles, towers, and conductors. Heavy rainfall and storm surge can flood substations and generating sites.

Vegetation contact and debris create additional failures. Historical evidence from the United States shows that tropical cyclones, thunderstorms, and winter storms account for most major weather-related interruptions (Shield et al., 2021). Hurricane outage risk is sensitive to uncertainty in future storm frequency and to the spatial configuration of the distribution system (Alemazkoor et al., 2020). Utility data from Japan show that restoration time rises with wind intensity and the geographic extent of damage (Li et al., 2025).

A national generation response is not guaranteed. Local network failures may disconnect customers, while large plants continue to produce. Generation can be reduced in the affected area but replaced by other domestic plants or imports. Monthly aggregation further dilutes outages that last several hours or days. High-frequency county-level data in China find that strong wind and rainstorms increase the frequency and duration of outages (Wang et al., 2025). Cascading models likewise show large local and system-wide consequences when critical network components fail (Xu et al., 2025a). These findings support a negative local outage hypothesis but do not determine the sign of national monthly generation.

Spatial exposure is necessary because a storm crossing national territory may remain far from electricity infrastructure. The analysis therefore weights exposure by the share of mapped national generating capacity near a qualifying track. The expected aggregate coefficient is negative, although monthly national generation may be too coarse to detect a short local interruption.

H3. A larger share of national generating capacity located within 250 km of a qualifying tropical storm track reduces aggregate monthly electricity generation after controlling for country-specific seasonality and global year-month shocks.

Generation diversification, storage, and interconnection can reduce vulnerability when resource shortfalls are weakly correlated and electricity can move across locations. Their value is event-specific. Recent European evidence shows that the geopolitical energy shock of 2022 accelerated renewable electricity deployment, particularly in relatively fast-deploying solar and wind technologies, although increased capacity alone does not demonstrate resilience to climate-related disruptions (Vasylieva, Derkacz, et al., 2025). Complementary European evidence links renewable-energy innovation with stronger energy security and economic viability, although this relationship concerns structural energy-system transformation rather than short-run responses to climate hazards (Svazas et al., 2025). Short-duration batteries address intraday imbalance, whereas multi-day shortages require greater energy duration, firm backup, or wider interconnection (Dowling et al., 2020; Qu et al., 2025; Schill, 2020; Sepulveda et al., 2021; Stiewe et al., 2025; Zheng et al., 2024).

Network quality and institutional capacity also shape recovery. Transmission and distribution losses can signal technical weakness, congestion, theft, or poor maintenance, while governance affects investment planning, emergency coordination, procurement, and reliability enforcement (Fedajev et al., 2023; Lin & Okoye, 2023). These broad indicators cannot directly measure local outage restoration, but they provide exploratory context for cross-country heterogeneity.

The moderation hypotheses are stated in relation to the storm coefficient. A more diversified generation portfolio should make national generation less sensitive to the loss of any one exposed group of plants. Lower network losses should indicate a stronger grid and therefore a smaller negative effect. Greater government effectiveness should support faster coordination and restoration. These hypotheses concern the aggregate monthly response. They do not imply that the same variables eliminate local outages.

H4. Greater generation diversification weakens a negative storm effect. In the interaction model, this prediction requires a positive coefficient on the interaction between storm exposure and diversification.

H5. Weaker networks amplify a negative storm effect and stronger institutions attenuate it. The coefficient on the interaction between storm exposure and network losses is expected to be negative, whereas the coefficient on the interaction between storm exposure and government effectiveness is expected to be positive.

3. Materials and Methods

The empirical design uses two linked panels because the availability of climate and storm variables differs. The climate sample covers Australia, Brazil, Canada, China, Germany, Egypt, Spain, India, Japan, Kazakhstan, Nigeria, and South Africa. Each country contributes 84 monthly observations from January 2019 through December 2025. The resulting 1,008 observations provide climatic and structural diversity but do not constitute a representative global sample.

The storm panel begins with countries that have complete Ember data for the same 84 months and at least one geocoded plant. It contains 74 countries and 6,216 observations. The IBTrACS source contains 529 tropical systems that meet the 34-knot wind criterion during the study period. Under the preferred binary definition, 168 country-months across 27 countries have at least 2% of mapped capacity within 250 km of a qualifying track.

The unit of analysis is the country-month. This frequency identifies persistent demand, substitution, and aggregate generation responses while maintaining international coverage. It does not identify hourly scarcity, customer interruption, or restoration curves. The outcomes are log monthly demand, log total generation, log absolute fossil generation, and the inverse hyperbolic sine of net imports. Absolute fossil generation replaces the fossil share in the main hydropower specification to avoid a mechanical increase due to lower hydro output. Data sources and variable construction are summarized in Table 1.

Table 1. Data sources and variable construction

Block	Source	Frequency	Use
Electricity outcomes	Ember monthly electricity data	Country-month	Demand, total generation, absolute fossil generation, hydro, and net imports
Temperature	CRU TS v4.10	Country-month	Mean temperature, historical anomaly, local P90 indicator, and threshold exposure
Tropical storms	NOAA IBTrACS v04r01	Track observation	Location, time, wind speed, and proximity to mapped capacity
Power plants	Global Power Plant Database	Plant	Coordinates, technology, and capacity exposure weights
Network quality	World Development Indicators	Country-year	Transmission and distribution losses
Institutions	Worldwide Governance Indicators	Country-year	Government effectiveness and related measures

Note. All annual controls are matched to each month of the corresponding year. The storm exposure measure is constructed by spatially linking plant coordinates with IBTrACS tracks.

Heat exposure is measured in two ways. Monthly cooling-threshold exposure equals the positive difference between country-average monthly temperature and 18 °C. It is not labeled "cooling degree days" because it is based on monthly rather than daily temperatures. Monthly heating-threshold exposure is constructed symmetrically below 18 °C. The second heat indicator equals 1 when the temperature exceeds the country-specific 90th percentile for the same calendar month from 1991 to 2020. Temperature anomalies are calculated relative to the corresponding historical normal. The common threshold is retained for comparability. Its limitations across climates are addressed through the local percentile measure and country-specific seasonal effects (Harris et al., 2020).

The operational hydropower shortfall is constructed from hydro generation because a harmonized physical series for precipitation, river discharge, reservoir inflow, storage, and snowpack is not available for the full sample period. Log hydro generation is standardized within country and calendar month. The shortfall equals $\max(0, -z)$, where z is standardized log hydropower generation within country and calendar month. Long-run hydropower dependence is mean hydro generation divided by total generation. The interaction identifies whether the contemporaneous balancing response is larger where hydro is structurally important. The primary model uses all 12 countries and therefore does not rely on an arbitrary hydropower-share cutoff. Thresholds of 5, 10, and 15 percent are retained only as sensitivity checks. Since the shortfall is derived from an electricity outcome, the estimates reflect descriptive substitution relationships rather than causal drought effects.

Storm exposure uses IBTrACS points with sustained wind of at least 34 knots. Track points are linked to power plants by great-circle distance. National exposed capacity is the sum of mapped capacity within 150 km, 250 km, or 350 km divided by total mapped capacity. The continuously exposed capacity percentage at 250 km is the primary variable. Binary indicators require at least 1%, 2%, 5%, or 10% exposure. Event-time estimates retain only isolated exposure months with no qualifying event during the preceding or following two months. Lead and lag indicators are derived from isolated events, so their estimation windows do not overlap. The resulting

event model contains 63 isolated exposure months in 25 countries. The Global Power Plant Database contains 34,936 plants in the supplied file. Its coordinates provide a transparent exposure weight but do not measure transmission lines, substations, or customer density.

Generation diversification equals one minus the Herfindahl index of hydro, wind, solar, nuclear, coal, and gas generation shares. It is omitted from baseline heat and storm models because contemporaneous generation composition may respond to climate exposure. The heat robustness model includes current diversification. The H4 interaction uses each country's mean diversification in 2019 and is estimated over the period 2020 to 2025. The H5 interactions use one-year-lagged network losses and government effectiveness. Network losses equal transmission and distribution losses divided by output, and government effectiveness is the Worldwide Governance Indicators estimate.

The baseline heat model relates log monthly demand to monthly cooling-threshold exposure and monthly heating-threshold exposure. Alternative models use the local 90th-percentile indicator, add current diversification only as a heat robustness check, include country-year effects, or include country-specific linear trends. The hydropower models relate absolute fossil generation, transformed net imports, and total generation to operational shortfall, its interaction with long-run hydropower dependence, and monthly cooling-threshold exposure. The primary hydropower sample contains all 12 countries. Storm models use continuous exposed capacity as the primary variable and binary thresholds as sensitivity checks. The baseline storm specification contains only storm exposure, country-by-calendar-month effects, and global year-month effects. Potentially post-treatment hydropower shortfall and contemporaneous diversification are excluded.

The empirical models are summarized by four compact equations.

$$\ln D_{it} = \beta_1 H_{it} + \beta_2 W_{it} + \alpha_{im} + \lambda_t + \varepsilon_{it} \quad (1)$$

$$Y_{it} = \beta_1 S_{it} + \beta_2 (S_{it} \times h_i) + \beta_3 C_{it} + \alpha_{im} + \lambda_t + \varepsilon_{it} \quad (2)$$

$$\ln G_{it} = \beta_1 X_{it} + \alpha_{im} + \lambda_t + \varepsilon_{it} \quad (3)$$

$$\ln G_{it} = \beta_1 X_{it} + \beta_2 M^*_{it} + \beta_3 (X_{it} \times M^*_{it}) + \alpha_{im} + \lambda_t + \varepsilon_{it} \quad (4)$$

In equation (1), D_it is monthly electricity demand, H_it denotes monthly cooling-threshold exposure or the local Hot P90 indicator, and W_it denotes heating-threshold exposure. In equation (2), S_it is operational hydropower shortfall, h_i is long-run hydropower dependence, and C_it is monthly cooling-threshold exposure. Y_it sequentially denotes log absolute fossil generation, the inverse hyperbolic sine of net imports, and log total generation. In equation (3), G_it is monthly generation and X_it is storm exposure. Equation (4) adds a predetermined moderator, using mean 2019 diversification or a one-year-lagged institutional indicator. The term alpha_im denotes country-by-calendar-month fixed effects, and lambda_t denotes global year-month fixed effects. Country-year effects and country-specific trends are introduced only in the stated robustness models.

Identification comes from within-country deviations for the same calendar month across years. Standard errors are clustered by country, and two-way clustering by country and global year-month is reported as a robustness check (Cameron et al., 2011). The climate and primary hydropower models contain 12 clusters. Main small-sample p-values use 999 restricted-residual wild-cluster bootstrap replications under the null and the Webb six-point weight distribution (Webb, 2023). Recent evidence supports the use of bootstrap and jackknife procedures when cluster counts are small or uneven (MacKinnon et al., 2023). Holm correction is applied to seven prespecified primary tests. Webb p-values are used for H1 and the two H2 outcomes; country-clustered p-values are used for H3 to H5.

The design is not a treatment-control experiment. Short-run heat and storm exposure are plausibly external to electricity decisions, but country-average monthly temperature remains a coarse measure. The hydropower shortfall is explicitly endogenous to the power balance and should not be interpreted causally. National monthly generation is treated as an observable aggregate response rather than a complete measure of reliability. Direct reliability claims would require SAIDI, SAIFI, energy not supplied, forced-capacity data, or customer interruption records. Descriptive statistics for the climate panel are reported in Table 2. The sample contains large differences in system scale and generation structure. Average monthly demand ranges from 2.5 TWh in Nigeria to 732 TWh in China. Mean hydropower share exceeds 0.58 in Brazil and Canada, while it is below 0.04 in Germany and

South Africa. Average network losses are below five percent in Australia, Canada, China, Germany, and Japan but exceed 14 percent in Brazil, Egypt, India, and Nigeria. These differences motivate the interaction models rather than a single homogeneous climate coefficient.

Table 2. Descriptive statistics for the climate panel

Variable	N	Mean	SD	Minimum	Maximum
Monthly demand, TWh	1,008	98.335	196.900	0.880	1,012.700
Monthly generation, TWh	1,008	98.856	197.184	0.880	1,014.530
Temperature, °C	1,008	16.153	11.527	-23.200	32.000
Temperature anomaly, °C	1,008	0.567	0.987	-3.913	5.607
Monthly cooling-threshold exposure	1,008	3.536	4.155	0.000	14.000
Operational hydropower shortfall	1,008	0.419	0.838	0.000	13.757
Fossil generation, TWh	1,008	59.507	128.682	0.660	607.740
Net imports, TWh	1,008	-0.521	1.343	-7.200	5.510
Hydropower share	1,008	0.179	0.199	0.001	0.735
Generation diversification	1,008	0.564	0.177	0.155	0.862
Network losses, percent	1,008	9.577	5.362	3.422	21.949
Government effectiveness	1,008	0.675	0.926	-1.057	2.088

Note. The climate panel contains 12 countries and 84 months per country. Hydropower shortfall is an operational output-based measure. Shares range from zero to one.

The sample contains large differences in system scale and generation structure. Average monthly demand ranges from 2.5 TWh in Nigeria to 732 TWh in China. Mean hydropower share exceeds 0.58 in Brazil and Canada, while it is below 0.04 in Germany and South Africa. Average network losses are below five percent in Australia, Canada, China, Germany, and Japan but exceed 14 percent in Brazil, Egypt, India, and Nigeria. These differences motivate the interaction models rather than a single homogeneous climate coefficient.

4. Results

Results are organized around the three climate exposures and the subsequent moderation tests. The heat models assess persistent demand responses, the hydropower models examine contemporaneous balancing through fossil generation and net imports, and the storm models evaluate whether infrastructure exposure is visible in national monthly generation. The final estimates test whether generation diversification, network losses, and government effectiveness alter the storm association. The temperature-demand estimates are presented in Table 3.

Table 3. Temperature exposure and monthly electricity demand

Statistic	M1 Baseline	M2 Hot P90	M3 Country-year FE	M4 Country trends	M5 Diversification
Key exposure coefficient	0.0262	0.0244	0.0209	0.0236	0.0255
Country-clustered SE	(0.0067)	(0.0070)	(0.0048)	(0.0049)	(0.0070)
Country-clustered p-value	0.002	0.005	0.001	0.001	0.004
Webb p-value	0.004	0.002	Not reported	Not reported	Not reported
Two-way clustered p-value	< 0.001	0.001	< 0.001	< 0.001	< 0.001
Observations	1,008	1,008	1,008	1,008	1,008

Countries	12	12	12	12	12
Within R^2	0.033	0.024	0.045	0.055	0.036
Country-by-calendar-month FE	Yes	Yes	Yes	Yes	Yes
Global year-month FE	Yes	Yes	Yes	Yes	Yes

Note. The dependent variable is log monthly electricity demand. Country-by-calendar-month and global year-month effects are included in every model. M3 adds country-year effects. M4 adds country-specific trends. M5 adds contemporaneous generation diversification. Webb p-values are reported for M1 and M2 and use 999 restricted-residual replications.

The baseline estimate supports H1. The monthly cooling-threshold coefficient is 0.0262. Its country-clustered p-value is 0.002, its Webb p-value is 0.004, and its Holm-adjusted primary p-value is 0.028. An additional degree above 18 °C is associated with approximately a 2.62 percent increase in monthly demand. The estimate remains positive with country-year effects, country-specific trends, two-way clustering, and contemporaneous diversification.

The locally defined heat indicator gives the same conclusion. Demand is 2.44 percent higher in months above the country and calendar-month 90th percentile. Its Webb p-value is 0.002. Leave-one-country-out estimates for the continuous exposure range from 0.0210 to 0.0292. The result, therefore, does not depend on a single large economy or a single climatic region. The model with contemporaneous diversification is retained only as a robustness check and produces a similar coefficient of 0.0255. Figure 1 displays the estimated demand response and its confidence bounds.

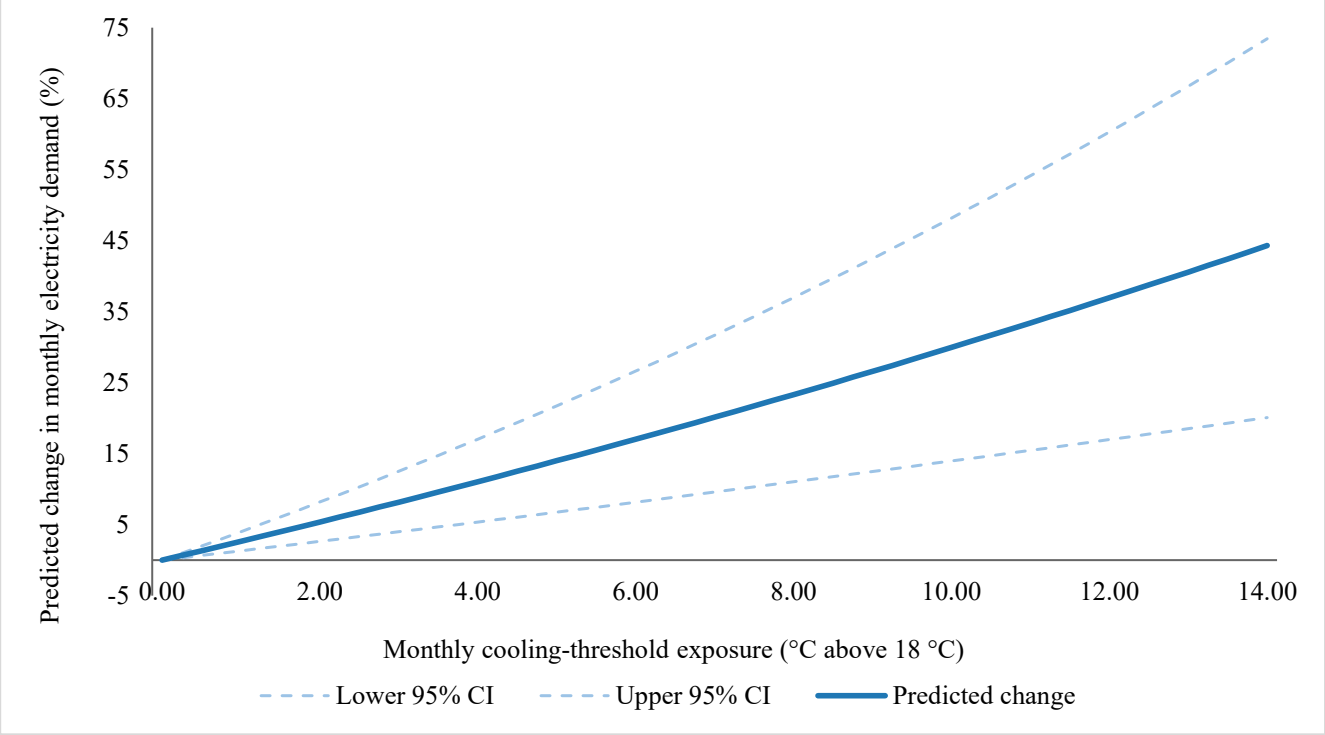


Fig. 1 Estimated demand response to monthly cooling-threshold exposure

Note. The solid line shows the predicted change in demand from M1. Dashed lines show the 95 percent country-clustered confidence bounds.

The heat results provide the clearest monthly signal, but they capture only the demand side of climate stress. The analysis next turns to operational hydropower shortfalls and examines whether systems with greater hydropower dependence compensate through higher fossil generation or net imports. The hydropower estimates and sensitivity checks are reported in Table 4.

Table 4. Operational hydropower shortfalls and absolute balancing outcomes

Statistic	M1 Fossil volume	M2 Net imports	M3 Total generation
Shortfall × hydro dependence	0.1913	0.8679	-0.0684
Country-clustered SE	(0.1239)	(0.3074)	(0.0270)
Country-clustered p-value	0.151	0.017	0.028
Webb p-value	0.112	0.292	0.014
Two-way clustered p-value	0.126	0.005	0.011
Observations	1,008	1,008	1,008
Countries	12	12	12
Within R^2	0.077	0.131	0.102
Country-by-calendar-month FE	Yes	Yes	Yes
Global year-month FE	Yes	Yes	Yes

Note. The primary sample contains all 12 climate-panel countries. The key coefficient is the product of operational shortfall and long-run hydropower dependence. Fossil generation and total generation are logged. Net imports use the inverse hyperbolic sine transformation. Webb p-values use 999 restricted-residual replications. All specifications additionally control for monthly cooling-threshold exposure. Threshold samples are treated only as sensitivity checks.

In the full 12-country sample, the shortfall interaction is 0.1913 for absolute fossil generation. Its country-clustered p-value is 0.151 and its Webb p-value is 0.112. The net-import interaction is 0.8679. Conventional country clustering gives a p-value of 0.017, but the Webb p-value is 0.292. The total-generation interaction is negative. Because the shortfall is constructed from low hydro output, that coefficient is partly definitional and is not treated as independent causal evidence. Total generation is a diagnostic outcome and is excluded from H2 and the Holm multiple-testing family.

H2 is not statistically supported under the prespecified small-cluster standard. The Holm-adjusted p-values are 0.672 for fossil generation and 1.000 for net imports. Restricting the sample to systems with mean hydropower shares above 5, 10, or 15 percent leaves the fossil and import interactions positive, but Webb p-values range from 0.103 to 0.516 for fossil generation and from 0.067 to 0.245 for net imports. The 15 percent specification contains only three countries and is interpreted as diagnostic. The evidence therefore describes contemporaneous balancing patterns rather than a causal response to physical drought. The subsequent storm-exposure estimates are presented in Table 5.

Table 5. Tropical storm exposure and aggregate monthly generation

Specification	Coefficient	SE	Country p-value	Two-way p-value	N
Continuous 150 km	0.00037	(0.00032)	0.244	0.178	6,216
Continuous 250 km	0.00023	(0.00025)	0.349	0.341	6,216
Continuous 350 km	0.00022	(0.00017)	0.185	0.169	6,216
Binary 1 percent	0.00193	(0.00770)	0.803	0.807	6,216
Binary 2 percent	0.00333	(0.00855)	0.698	0.718	6,216
Binary 5 percent	0.00612	(0.00953)	0.523	0.581	6,216
Binary 10 percent	0.00588	(0.01003)	0.559	0.626	6,216
Binary 2 percent with country-year FE	0.00514	(0.00524)	0.330	0.299	6,216
Binary 2 percent with country trends	0.00854	(0.00778)	0.276	0.272	6,216

Note. The continuous coefficient is reported per one percentage point of mapped national capacity within the stated radius. Binary models compare exposed and unexposed months at a 250 km resolution. Baseline models include only storm exposure, country-by-calendar-month effects, and global year-month effects. The final two

rows add country-year effects or country-specific trends. Contemporaneous hydropower shortfall and generation diversification are excluded because they may respond to the storm.

After potentially post-treatment controls are removed, the continuous 250 km coefficient is 0.00023 per exposed-capacity percentage point, with a country-clustered p-value of 0.349. Coefficients at 150 km and 350 km are also small and statistically imprecise. Binary thresholds from 1 to 10 percent produce estimates between 0.19 and 0.61 percent. H3 is not supported. Figure 2 compares the alternative exposed-capacity thresholds.

The conclusion is unchanged with country-year effects, country-specific trends, two-way clustering, and leave-one-country-out analysis. The continuous 250 km leave-one-country-out coefficients range from 0.00010 to 0.00040. The isolated event-time model excludes exposure months that have another event within 2 months on either side. Estimated generation is 0.58 percent lower in the month before, 0.89 percent lower in the exposure month, and 1.33 percent lower in the following month. All three country-clustered p-values exceed 0.20. Monthly national generation therefore remains too aggregated to identify a common short-lived storm effect.

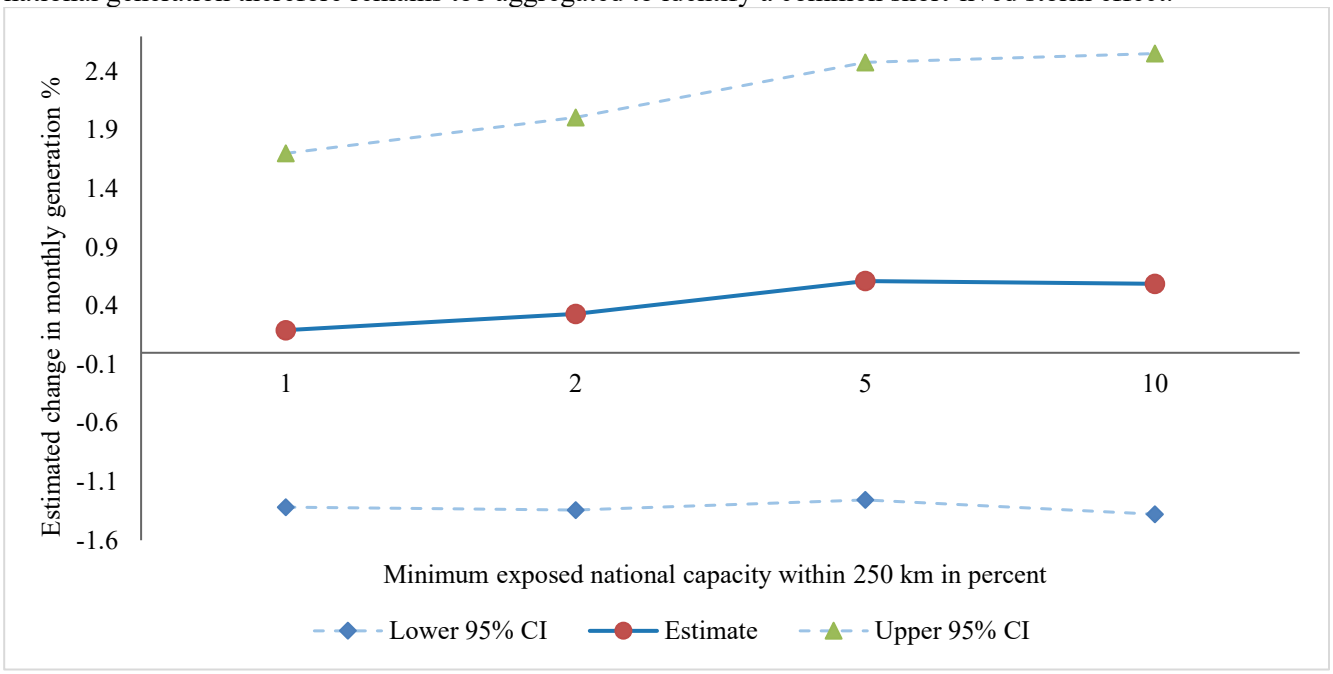


Fig. 2 *Storm coefficients under alternative exposed-capacity thresholds*

Note. Points show percentage changes in monthly generation for binary thresholds at 250 km. Dashed lines show the 95 percent country-clustered confidence bounds.

The threshold estimates do not reveal a statistically precise contemporaneous generation response. To examine whether the effect emerges around the timing of isolated storms, the event-time analysis compares generation in the month before, during, and after exposure. Figure 3 presents the corresponding event-time coefficients.

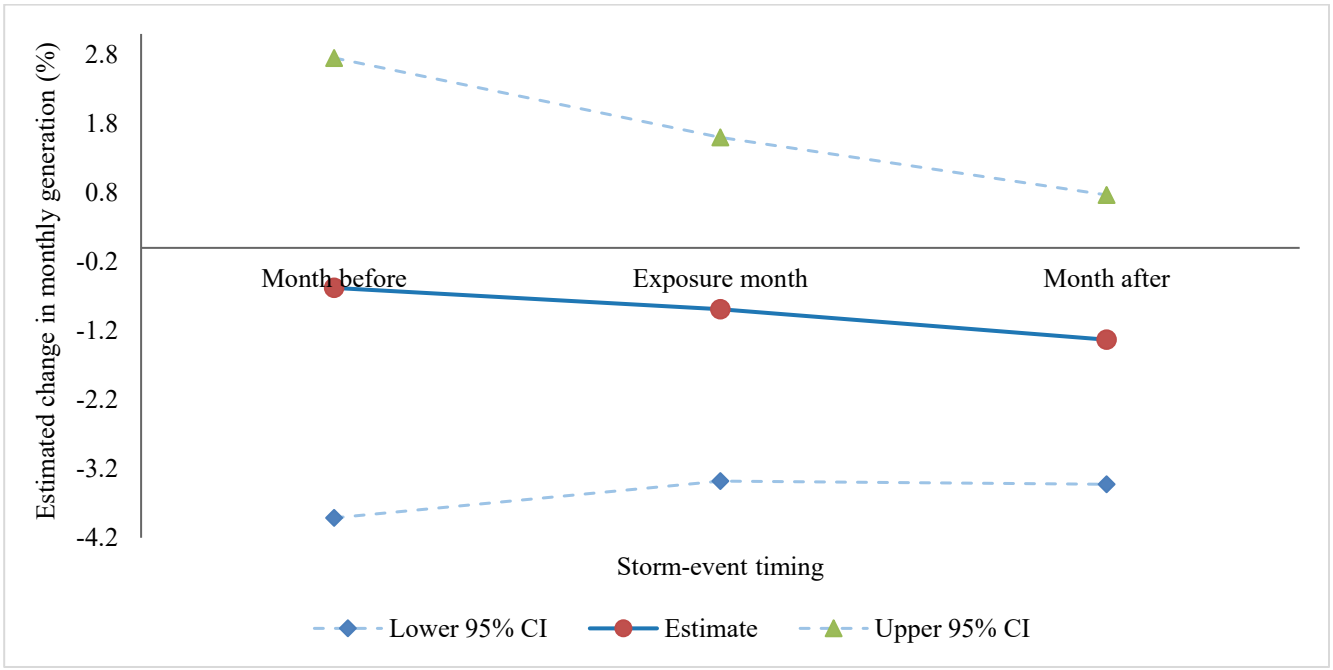


Fig. 3 Aggregate generation before, during, and after storm exposure

Note. Points show coefficients for isolated storm events with no other qualifying event in the preceding or following two months. The three estimation windows do not overlap. Dashed lines show the 95 percent country-clustered confidence bounds.

The event-time estimates likewise provide no statistically precise evidence of a common national generation response around isolated storm exposure. The analysis therefore turns to the prespecified moderation tests and summarizes the evidence across all hypotheses. Table 6 reports the moderation estimates and summarizes the conclusions for all hypotheses.

Table 6. Moderating effects and hypothesis conclusions

Test	Expected sign	Coefficient	Primary p-value	Two-way p-value	Holm-adjusted p-value	Conclusion
H1 heat	Positive	0.0262	0.004	< 0.001	0.028	Supported
H2 fossil volume	Positive	0.1913	0.112	0.126	0.672	Not supported
H2 net imports	Positive	0.8679	0.292	0.005	1.000	Not supported
H3 storm exposure	Negative	0.00023	0.349	0.341	1.000	Not supported
H4 pre-period diversification	Positive	0.00072	0.323	0.018	1.000	Predicted sign, not supported
H5 lagged network losses	Negative	0.00001	0.905	0.903	1.000	Opposite sign, not supported
H5 lagged government effectiveness	Positive	0.00026	0.512	0.542	1.000	Predicted sign, not supported

Note. The H4 moderator is mean generation diversification during 2019, and the model is estimated over 2020 to 2025. H5 uses one-year-lagged network losses and government effectiveness. Primary p-values use Webb inference for H1 and H2, and country clustering for H3-H5. Holm adjustment is applied to the seven prespecified primary p-values. Interaction models remain informative when the average storm coefficient is near zero because heterogeneous positive and negative effects may offset across systems.

The interaction between storm exposure and pre-period diversification has the predicted positive sign, but its country-clustered p-value is 0.323, and its Holm-adjusted p-value is 1.000. The network-loss interaction has

the opposite sign and a p-value of 0.905, while the government-effectiveness interaction has the predicted positive sign and a p-value of 0.512. H4 and H5 are therefore not supported. After Holm correction, H1 is the only supported hypothesis.

5. Discussion

The central result is not that heat matters while hydropower shortfalls and storms do not. It is that different hazards leave different empirical signatures in aggregate power-system data. Heat is the only exposure that produces a robust national monthly signal because its demand effect persists across much of the observation period. Operational hydropower shortfalls reveal contemporaneous balancing but cannot identify a meteorological drought effect, while tropical-storm damage is often too localized and short-lived to appear in national monthly generation. The asymmetry is therefore a substantive finding about hazard measurement. Resilience assessment must link each physical hazard to an outcome observed at the spatial and temporal scale at which disruption and recovery occur.

The heat result is the strongest empirical finding and the clearest adaptation signal. Monthly cooling-threshold exposure does not claim the daily precision of conventional cooling degree days, and the common 18 °C threshold remains imperfect across climates and income levels. Nevertheless, the country-specific 90th-percentile specification produces a similar conclusion. This consistency matters because heatwaves can simultaneously raise load, reduce generation availability, and increase local network vulnerability (Guddanti et al., 2025; Sergio & Colelli, 2025; Xu et al., 2025b). Adaptation plans based only on historical peak demand may therefore understate future adequacy requirements.

Heat-responsive planning advances both reliable energy access and climate adaptation. Efficient cooling, building insulation, demand response, and time-varying tariffs can reduce persistent warm-season load, while adequacy planning should account for correlated increases in demand and reductions in available capacity during extreme heat (Borenstein & Bushnell, 2022; Denholm et al., 2021; Schill, 2020). Smart energy transformation can improve efficiency, reliability, and sustainability by coordinating production, consumption, and infrastructure management (Chygryn et al., 2026). These measures connect SDG 7 and SDG 13 directly: expanding access and decarbonizing supply will not be sustainable if systems cannot maintain affordable service under intensifying heat. Resilience metrics that incorporate backup investment during extreme weather point in the same direction (Grochowicz et al., 2026).

Hydrological adaptation requires a different evidence base. The operational shortfall used here begins after low hydro output is already observed and is therefore unsuitable as an independent physical drought treatment. A stronger design would connect basin precipitation, runoff, snowpack, reservoir inflow, and storage to reservoir and run-of-river plants. The CRU data support transparent temperature measurement but do not replace plant-weighted hydrology (Harris et al., 2020). This limitation has direct planning implications: without meteorology-to-generation validation, governments may misjudge replacement capacity, reservoir coordination, import requirements, and the risk of compound renewable-energy droughts across technologies and seasons (van der Most et al., 2022).

The storm null result is most informative as an adaptation-measurement result. High-frequency studies show that storms increase outage frequency, duration, and restoration burdens (Shield et al., 2021; Li et al., 2025; Wang et al., 2025), while cascading models demonstrate that component location and network topology determine whether failures propagate (Xu et al., 2025a). A national monthly generation series can remain stable when unaffected plants increase output, imports rise, or service is restored before month-end. Consequently, a near-zero aggregate coefficient should not be used to conclude that network hardening, distributed backup, spare equipment, or mutual-aid capacity is unnecessary.

Adaptation assessment should preserve the full chain from hazard to infrastructure exposure, component failure, customer interruption, substitution, restoration, and economic loss. National production lies near the end of this chain. It indicates whether the energy balance was restored, not whether service remained continuous or whether vulnerable consumers experienced disproportionate losses. The development consequences depend on interruption duration, the customers and essential services affected, and access to backup power (Aweke & Navrud, 2022; Chen et al., 2023; Sue Wing et al., 2025). Resilience monitoring that omits these dimensions can overstate progress toward reliable and inclusive energy access.

Storage and interconnection remain central adaptation instruments, but their design must reflect hazard duration. Short-duration batteries can address intraday imbalance and support critical loads, whereas multi-day events require greater energy duration, firm backup, or wider interconnection. Their value depends on regional correlation, event duration, and market design (Dowling et al., 2020; López Prol & Schill, 2021; Ruhnau & Qvist, 2022; Sepulveda et al., 2021). Recent evidence also shows that storage and interconnection can preserve the value of renewables without eliminating the need for firm capacity (Stiewe et al., 2025). Sustainable power-sector transformation therefore requires resilience portfolios rather than reliance on a single technology.

The unsupported institutional interactions also carry a measurement lesson. Broad annual indicators of network losses and government effectiveness may be too coarse to represent restoration planning, spare-equipment availability, mutual-aid agreements, distribution-network maintenance, procurement capacity, or emergency coordination. Their statistical imprecision does not demonstrate that institutions are irrelevant; it indicates that institutional adaptation capacity should be measured closer to the operational mechanisms through which recovery occurs.

The cross-country design has both policy value and clear limitations. It shows where harmonized monthly data support comparative adaptation assessment and where they do not. Broader energy-security research similarly treats resilience as a multidimensional construct requiring a portfolio of indicators rather than a single aggregate output measure (Kharazishvili et al., 2025). Temperature and demand can be linked consistently, while output-based hydropower shortfalls describe balancing without identifying physical drought. Track-to-plant exposure improves on countrywide storm assignment but does not measure lines, substations, customer density, or interruption duration. The climate sample contains only 12 countries selected by data availability, and country-average temperature understates urban and population-weighted heat. The broader storm panel relies on a static plant database, while plant proximity is not equivalent to network exposure. These constraints limit generalization but clarify the data architecture needed for more credible adaptation monitoring.

Future research should combine plant-level generation and forced-outage records with daily population-weighted temperature, basin runoff, reservoir storage, and detailed hazard footprints. Distribution-network records are essential because many storm failures occur below the transmission level. Event studies should use hourly or daily interruption outcomes and restoration curves, while economic analysis should link outage duration to productivity, welfare, essential services, and exposure inequality. Research on islandable microgrids similarly emphasizes that reliable low-carbon systems require high-granularity data, short-horizon forecasting, and standardized evaluation protocols (Wojciechowski et al., 2025). This agenda would connect physical resilience more directly with inclusive sustainable-development outcomes.

6. Conclusion

This study shows that climate hazards cannot be evaluated through a single aggregate electricity indicator. Monthly data identify a robust positive demand response to heat but no robust fossil-generation, import, or national-generation responses to operational hydropower shortfalls and tropical storms. The findings do not imply an absence of physical impacts. Rather, national monthly data capture persistent system pressure more effectively than short and geographically concentrated service interruptions.

The central contribution is to connect climate-risk measurement with adaptation strategy. A near-zero storm coefficient in national generation is not evidence of a near-zero outage effect. Indicators used to guide resilient energy investment must correspond to the physical channel, location, and duration of each hazard. Without that alignment, aggregate stability may conceal service disruption and unequal recovery.

The policy implications are hazard-specific but jointly support sustainable development. Heat adaptation requires efficient cooling, building performance, demand response, and temperature-aware adequacy planning. Hydrological adaptation requires basin information, reservoir coordination, interconnection, storage, and replacement plans. Storm adaptation requires network hardening, distributed backup, spare equipment, and rapid restoration. Progress toward SDGs 7 and 13 consequently depends not only on expanding and decarbonizing electricity supply but also on measurement systems that link hazards with component exposure, service interruption, balancing, recovery, and economic loss.

References

Abeberese, A. B., Ackah, C. G., & Asuming, P. O. (2021). Productivity losses and firm responses to electricity shortages: Evidence from Ghana. *The World Bank Economic Review, 35*(1), 1–18. https://doi.org/10.1093/wber/lhz027

Alemazkoor, N., Rachunok, B., Chavas, D. R., Staid, A., Louhghalam, A., Nateghi, R., & Tootkaboni, M. (2020). Hurricane-induced power outage risk under climate change is primarily driven by the uncertainty in projections of future hurricane frequency. *Scientific Reports, 10*, 15270. https://doi.org/10.1038/s41598-020-72207-z

Aweke, A. T., & Navrud, S. (2022). Valuing energy poverty costs: Household welfare loss from electricity blackouts in developing countries. *Energy Economics, 109*, 105943. https://doi.org/10.1016/j.eneco.2022.105943

Borenstein, S., & Bushnell, J. B. (2022). Do two electricity pricing wrongs make a right? Cost recovery, externalities, and efficiency. *American Economic Journal: Economic Policy, 14*(4), 80–110. https://doi.org/10.1257/pol.20190758

Byers, L., Friedrich, J., Hennig, R., Kressig, A., Li, X., McCormick, C., & Valeri, L. M. (2019). *A global database of power plants*. World Resources Institute.

Cameron, A. C., Gelbach, J. B., & Miller, D. L. (2011). Robust inference with multiway clustering. *Journal of Business & Economic Statistics, 29*(2), 238–249. https://doi.org/10.1198/jbes.2010.07136

Chen, H., Jin, L., Wang, M., Guo, L., & Wu, J. (2023). How will power outages affect national economic growth? Evidence from 152 countries. *Energy Economics, 126*, 107055. https://doi.org/10.1016/j.eneco.2023.107055

Chygryn, O., Ziabina, Y., Štreimikienė, D., & Bilan, Y. (2026). Outcomes of innovative technologies and smart transformation of the energy sector. *Journal of Innovation & Knowledge, 12*, 100910. https://doi.org/10.1016/j.jik.2025.100910

Denholm, P., Arent, D. J., Baldwin, S. F., Bilello, D. E., Brinkman, G. L., Cochran, J. M., Cole, W. J., Frew, B., Gevorgian, V., Heeter, J., Hodge, B. M. S., Kroposki, B., Mai, T., O'Malley, M. J., Palmintier, B., Steinberg, D., & Zhang, Y. (2021). The challenges of achieving a 100% renewable electricity system in the United States. *Joule, 5*(6), 1331–1352. https://doi.org/10.1016/j.joule.2021.03.028

Dowling, J. A., Rinaldi, K. Z., Ruggles, T. H., Davis, S. J., Yuan, M., Tong, F., Lewis, N. S., & Caldeira, K. (2020). Role of long-duration energy storage in variable renewable electricity systems. *Joule, 4*(9), 1907–1928. https://doi.org/10.1016/j.joule.2020.07.007

Elliott, R. J. R., Nguyen-Tien, V., & Strobl, E. A. (2021). Power outages and firm performance: A hydro-IV approach for a single electricity grid. *Energy Economics, 103*, 105571. https://doi.org/10.1016/j.eneco.2021.105571

Ember. (2026). *Monthly electricity data* [Data set]. Retrieved July 28, 2026, from https://ember-energy.org/data/api/

Fedajev, A., Mitić, P., Kojić, M., & Radulescu, M. (2023). Driving industrial and economic growth in Central and Eastern Europe: The role of electricity infrastructure and renewable energy. *Utilities Policy, 85*, 101683. https://doi.org/10.1016/j.jup.2023.101683

Grochowicz, A., Bloomfield, H. C., & Victoria, M. (2026). Resilience metrics to guide back-up investments in the power system during extreme weather. *Nature Sustainability*. Advance online publication. https://doi.org/10.1038/s41893-026-01897-6

Guddanti, K. P., Chen, L., Weng, Y., & Yu, Y. (2025). Vulnerability of power distribution networks to local temperature changes induced by global climate change. *Nature Communications, 16*, 5116. https://doi.org/10.1038/s41467-025-59749-4

Harris, I., Osborn, T. J., Jones, P., & Lister, D. (2020). Version 4 of the CRU TS monthly high-resolution gridded multivariate climate dataset. *Scientific Data, 7*, 109. https://doi.org/10.1038/s41597-020-0453-3

Kharazishvili, Y., Bilan, Y., Sukhodolia, O., Grishnova, O., & Mishchuk, H. (2025). Scientific and strategic foresighting: The trajectory of sustainable development on the example of Ukraine's energy security. *Sustainable Futures, 9*, 100580. https://doi.org/10.1016/j.sftr.2025.100580

Knapp, K. R., Kruk, M. C., Levinson, D. H., Diamond, H. J., & Neumann, C. J. (2010). The International Best Track Archive for Climate Stewardship. *Bulletin of the American Meteorological Society, 91*(3), 363–376. https://doi.org/10.1175/2009BAMS2755.1

Li, Y., Xiao, F., Zhang, X., Gao, W., Ruan, Y., Zhou, N., & Kammen, D. M. (2025). Extreme typhoon events trigger long-lasting power outages and require demand-side solutions to enhance energy resiliency. *Communications Earth & Environment, 6*, 136. https://doi.org/10.1038/s43247-025-02126-2

Lin, B., & Okoye, J. O. (2023). Towards renewable energy generation and low greenhouse gas emission in high-income countries: Performance of financial development and governance. *Renewable Energy, 215*, 118931. https://doi.org/10.1016/j.renene.2023.118931

López Prol, J., & Schill, W. P. (2021). The economics of variable renewable energy and electricity storage. *Annual Review of Resource Economics, 13*, 443–467. https://doi.org/10.1146/annurev-resource-101620-081246

MacKinnon, J. G., Nielsen, M. Ø., & Webb, M. D. (2023). Fast and reliable jackknife and bootstrap methods for cluster-robust inference. *Journal of Applied Econometrics, 38*(5), 671–694. https://doi.org/10.1002/jae.2969

Perera, A. T. D., Nik, V. M., Chen, D., Scartezzini, J. L., & Hong, T. (2020). Quantifying the impacts of climate change and extreme climate events on energy systems. *Nature Energy, 5*, 150–159. https://doi.org/10.1038/s41560-020-0558-0

Qiu, M., Ratledge, N., Azevedo, I. M. L., Diffenbaugh, N. S., & Burke, M. (2023). Drought impacts on the electricity system, emissions, and air quality in the western United States. *Proceedings of the National Academy of Sciences, 120*(28), e2300395120. https://doi.org/10.1073/pnas.2300395120

Qu, M., Shen, L., Zeng, Z., Yang, B., Zhong, H., Yang, X., & Lu, X. (2025). Prolonged wind droughts in a warming climate threaten global wind power security. *Nature Climate Change, 15*, 842–849. https://doi.org/10.1038/s41558-025-02387-x

Ruhnau, O., & Qvist, S. (2022). Storage requirements in a 100% renewable electricity system: Extreme events and inter-annual variability. *Environmental Research Letters, 17*(4), 044018. https://doi.org/10.1088/1748-9326/ac4dc8

Schill, W. P. (2020). Electricity storage and the renewable energy transition. *Joule, 4*(10), 2059–2064. https://doi.org/10.1016/j.joule.2020.07.022

Sepulveda, N. A., Jenkins, J. D., Edington, A., Mallapragada, D. S., & Lester, R. K. (2021). The design space for long-duration energy storage in decarbonized power systems. *Nature Energy, 6*(5), 506–516. https://doi.org/10.1038/s41560-021-00796-8

Sergio, A., & Colelli, F. P. (2025). Weather-induced power plant outages: Empirical evidence from hydro and thermal generators in Europe. *Energy Economics, 148*, 108549. https://doi.org/10.1016/j.eneco.2025.108549

Shahzad, A. A., Anwar, M. A., Arshed, N., & Bilan, Y. (2024). Nexus between economic growth, renewable energy and climate vulnerability: A global perspective using the EKC framework. *Renewable Energy, 237*, 121716. https://doi.org/10.1016/j.renene.2024.121716

Shen, J., Wang, Y., Lin, M., Cheng, C., Kazak, J. K., Wang, J., Guo, X., Li, X., Zhou, B., & Ge, L. (2025). Quantifying the impact of extreme weather on China's hydropower-wind-solar renewable energy system. *Nature Water, 3*, 415–429. https://doi.org/10.1038/s44221-025-00408-9

Shield, S. A., Quiring, S. M., Pino, J. V., & Buckstaff, K. (2021). Major impacts of weather events on the electrical power delivery system in the United States. *Energy, 218*, 119434. https://doi.org/10.1016/j.energy.2020.119434

Stiewe, C., Xu, A., Eicke, A., & Hirth, L. (2025). The value of variable renewables: Cannibalization, interconnection, and storage. *Energy Economics, 143*, 108251. https://doi.org/10.1016/j.eneco.2025.108251

Sue Wing, I., Larsen, P. H., Carvallo, J. P., Sanstad, A., Wei, D., Rose, A., Baik, S., Smith, J., Ramee, C., & Peterson, R. (2025). A method to estimate the economy-wide consequences of widespread, long duration electric power interruptions. *Nature Communications, 16*, 3335. https://doi.org/10.1038/s41467-025-58537-4

Svazas, M., Navickas, V., Paskevicius, R., Bilan, Y., & Shahzad, U. (2025). Energy security challenges in Europe: The importance of renewable energy innovations for economic viability after Russia Ukraine war. *Environment, Development and Sustainability*. Advance online publication. https://doi.org/10.1007/s10668-025-06163-x

van der Most, L., van der Wiel, K., Benders, R. M. J., Gerbens-Leenes, P. W., & Bintanja, R. (2024). Temporally compounding energy droughts in European electricity systems with hydropower. *Nature Energy, 9*, 1474–1484. https://doi.org/10.1038/s41560-024-01640-5

van der Most, L., van der Wiel, K., Bintanja, R., & Benders, R. M. J. (2022). Extreme events in the European renewable power system: Validation of a modelling framework to estimate renewable electricity production and demand from meteorological data. *Renewable and Sustainable Energy Reviews, 170*, 112987. https://doi.org/10.1016/j.rser.2022.112987

Vasylieva, T., Derkacz, A., Popp, J., & Horsch, A. (2025). From energy dependency to energy security: How the war in Ukraine accelerated renewable deployment in Europe. *Economics & Sociology, 18*(3), 229–253. https://doi.org/10.14254/2071-789X.2025/18-3/13

Vasylieva, T., Gutowski, P., & Smiech, L. (2025). Dynamic inflation responses to war-related electricity shocks: DTW-based evidence from European energy and renewables regimes. *Journal of International Studies, 18*(4), 180–203. https://doi.org/10.14254/2071-8330.2025/18-4/9

Wang, B., Shi, H., Qiu, Y. L., Deng, N., Nock, D., Shen, X., Wang, Z., & Wang, Y. D. (2025). Unequal power outages induced by natural disasters. *Nature Communications, 16*, 8947. https://doi.org/10.1038/s41467-025-64012-x

Webb, M. D. (2023). Reworking wild bootstrap-based inference for clustered errors. *Canadian Journal of Economics, 56*(3), 839–858. https://doi.org/10.1111/caje.12661

Wojciechowski, W., Niewiadomski, A., & Bilan, Y. (2025). Ecological and secure electricity microgrids: Monitoring and forecasting challenges. *Human Technology, 21*(3), 469–473. https://doi.org/10.14254/1795-6889.2024.21-3.0

World Bank. (2026a). *World Development Indicators* [Data set]. Retrieved July 28, 2026, from https://databank.worldbank.org/source/world-development-indicators

World Bank. (2026b). *Worldwide Governance Indicators* [Data set]. Retrieved July 28, 2026, from https://www.worldbank.org/en/publication/worldwide-governance-indicators

Xu, L., Lin, N., Poor, H. V., Xi, D., & Perera, A. T. D. (2025). Quantifying cascading power outages during climate extremes considering renewable energy integration. *Nature Communications, 16*, 2582. https://doi.org/10.1038/s41467-025-57565-4

Xu, X., He, S., Zhou, B., Wang, H., Jiang, H., Liu, C., Sun, B., Yin, T., & Yan, J. (2025). South European heatwaves and their impacts on the power system in 2022. *Journal of Geophysical Research: Atmospheres, 130*, e2024JD042310. https://doi.org/10.1029/2024JD042310

Zhao, J., Li, F., & Zhang, Q. (2024). Impacts of renewable energy resources on the weather vulnerability of power systems. *Nature Energy, 9*, 1407–1414. https://doi.org/10.1038/s41560-024-01652-1

Zheng, D., Tong, D., Davis, S. J., Qin, Y., Liu, Y., Xu, R., Yang, J., Yan, X., Geng, G., Che, H., & Zhang, Q. (2024). Climate change impacts on the extreme power shortage events of wind-solar supply systems worldwide during 1980 to 2022. *Nature Communications, 15*, 5225. https://doi.org/10.1038/s41467-024-48966-y

Statements and declarations

Funding. The authors received no specific funding for this research.

Competing interests. The authors declare that they have no competing interests.

Author contributions. All authors contributed to the study conception and design. Material preparation, data collection and analysis were performed by Behzod Tagaev, Yuriy Bilan and Dalia Streimikiene. The first draft of the manuscript was written by all authors, and all authors reviewed and approved the final manuscript.

Data availability. The analysis uses open or redistributable data from Ember (2026), CRU TS v4.10 and its country aggregates (Harris et al. 2020), the National Oceanic and Atmospheric Administration International Best Track Archive for Climate Stewardship (Knapp et al. 2010), the Global Power Plant Database (Byers et al. 2019), World Development Indicators (World Bank 2026a), and Worldwide Governance Indicators (World Bank 2026b). The replication package contains the analytical panels, variable-construction files, estimation code and model outputs and will be deposited in a public repository upon acceptance.

Ethics approval. This study used publicly available country-level and infrastructure data and did not involve human participants, animals or personally identifiable information. Ethics approval was therefore not required.

Consent to participate. Not applicable.

684 **Consent for publication**. All authors approved the final manuscript and consent to its publication.
685 1
686